# Magnetic properties of a $GdFe_5Al_7$ single crystal

D. I. Gorbunov,[1,2,3,*] A. V. Andreev,[1] and M. D. Kuz'min[4]

[1]*Institute of Physics, Academy of Sciences, Na Slovance 2, 182 21 Prague, Czech Republic*

[2]*Institute of Metal Physics, Ural Branch of Russian Academy of Sciences, Kovalevskaya 18, 620990 Ekaterinburg, Russia*

[3]*Department of Condensed Matter Physics, Charles University, Ke Karlovu 5, 121 16 Prague, Czech Republic*

[4]*Leibniz-Institut für Festkörper- und Werkstoffforschung, PF 270116, D-01171 Dresden, Germany*

(Received 24 April 2012; revised manuscript received 17 June 2012; published 9 July 2012)

Magnetic properties of a tetragonal intermetallic compound $GdFe_5Al_7$ have been studied on a single crystal in static magnetic fields up to 14 T. The system is a ferrimagnet ($T_C = 265$ K) and on this premises we succeeded in describing its low-temperature magnetization curves as well as the temperature dependence of the spontaneous magnetization. The compound is interesting in two ways: (i) the iron sublattice is diluted so heavily that it is close to the stability limit and cannot be regarded as saturated, (ii) at low temperatures the system is in a state of near compensation, that is, the sublattice moments, albeit distinct, are close in magnitude. The latter has several consequences. (i) The net spontaneous magnetization is small, $M_s = 0.58\ \mu_B$/f.u. at $T = 2$ K. (ii) The system is in the strong-anisotropy regime despite the weakness of its anisotropy (attributed entirely to the iron sublattice) in energy terms. (iii) A moderate field (∼7 T) applied in the easy direction [110] suffices to induce a phase transition into a noncollinear magnetic state.

DOI: 10.1103/PhysRevB.86.024407 PACS number(s): 75.30.Gw, 75.50.Gg

## I. INTRODUCTION

Ferrimagnetism is a complex phenomenon, so a quantitative study necessitates carefully selected model systems and special experimental conditions. A useful concept in this respect is that of rigid sublattices, whereby the sublattice moments retain their magnitude as they reorient themselves in a strong magnetic field. Experimentally, this is ensured by working at low (liquid He) temperature. (An added advantage of low temperature is that it helps to minimize the magnetocaloric effect.) In the case of ferrimagnetic $3d$-$4f$ intermetallics, it is rather obvious that a localized $4f$ moment seeing a molecular field $\sim 10^2$ T is fully saturated at $T \sim 4$ K. As regards the itinerant $3d$ sublattice, its susceptibility $\chi_{3d}$ does not vanish as $T \to 0$. Still, $\chi_{3d}$ is usually small and the approximation of rigid sublattices does hold. A key quantity in itinerant magnetism is the Stoner exchange parameter, which roughly has the same value for all late $3d$ elements, $I_{3d} \sim 0.6$ eV.[1] In magnetically ordered $3d$ systems the density of states at the Fermi level $D(E_F)$ has to be $\sim I_{3d}^{-1}$, therefore, for the Pauli susceptibility one has $\chi_{3d} \sim \mu_B^2 I_{3d}^{-1} \sim 1 \times 10^{-4}\ \mu_B$/T per atom. Thus, in a magnetic field $\lesssim 10^2$ T the increment of the $3d$ moment is $\lesssim 1 \times 10^{-2}\ \mu_B$/atom (i.e., less than 1%). This estimate may need to be increased several times on account of the so-called exchange enhancement. However, cases of very strong enhancement (one order of magnitude or more) are rare. A necessary condition is that the product $I_{3d} D(E_F)$ be very close to unity. Physically, in order for the rigid-sublattice approximation to break down, the system must be very close to Stoner's ordering threshold.

$RFe_5Al_7$ are just such systems. (Here R stands for a heavy rare earth, R = Gd-Tm.) They can be regarded as $RFe_{12}$ compounds with a heavily diluted iron sublattice. The crystal structure is of the $ThMn_{12}$ type (space group $I4/mmm$), where the R atoms reside on the $2a$ sites, while Fe and Al occupy the $8f$ and $8i$ sites, respectively. The excess Fe atoms share the $8j$ positions with Al. The dilution with Al is so heavy, that the ferrimagnetic order ($\boldsymbol{M}_{Fe} \uparrow\downarrow \boldsymbol{M}_R$), albeit stable, is on the verge of collapse. Regarded in isolation, the iron sublattice in $RFe_5Al_7$ does not fulfill the Stoner condition. Accordingly, no ferromagnetism is observed either in $YFe_5Al_7$ or in $LuFe_5Al_7$, even though a noncollinear antiferromagnetic ordering does take place.[2] It is the presence of magnetic rare earths that brings $RFe_5Al_7$ over the Stoner threshold, owing to the R-Fe exchange interaction. As a result, all iron spins are aligned and make a joint magnetic sublattice, the R atoms being polarized in the opposite sense.[3] The weakness of the R-Fe exchange in relation to the Fe-Fe one suggests that the iron sublattice in $RFe_5Al_7$ cannot be far from the Stoner threshold. It is therefore expected to possess a considerable susceptibility and cannot be regarded as rigid. Thus, the $RFe_5Al_7$ compounds are suitable objects for quantitative studies of ferrimagnets beyond the rigid-sublattice approximation.

Unlike other magnetic rare earths, Gd has $L = 0$ and its magnetic moment is not sensitive to the (unknown) crystal field. Therefore, $GdFe_5Al_7$ provides us with an opportunity to quantitatively describe the spontaneous magnetization. A major role in this description is played by the Gd-Fe exchange field, also obtainable from low-temperature magnetization curves. This enables us to check the consistency of the models describing the magnetic behavior in both limits, $T \to 0$, $H \neq 0$, and $H \to 0$, $T \neq 0$.

$GdFe_5Al_7$ is also interesting from another prospective: its low-temperature spontaneous magnetization turns out to be very small [see Eq. (1) below], which means a near compensation of the sublattice moments at low temperatures. One can expect unusual strong manifestations of the weak (in energy terms) magnetic anisotropy.

This paper is structured as follows. Upon a brief presentation of the experimental procedure (Sec. II) and results (Sec. III), the model is exposed in Sec. IV. This is followed by a discussion (Sec. V) and conclusions (Sec. VI). The Appendix demonstrates a way to reduce the model of Sec. IV to the standard model of rigid sublattices.

 

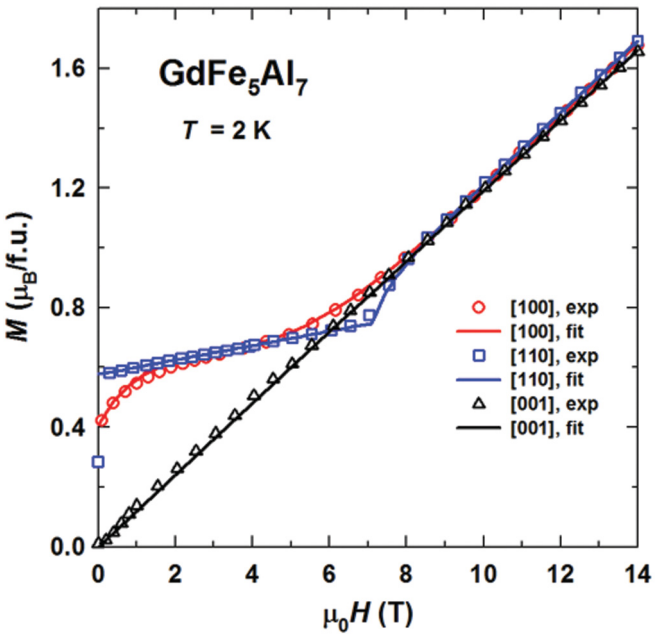


FIG. 1. (Color online) Magnetization isotherms measured along the principal axes of a $GdFe_5Al_7$ single crystal at 2 K. Symbols represent experiment; lines represent fits (see below).

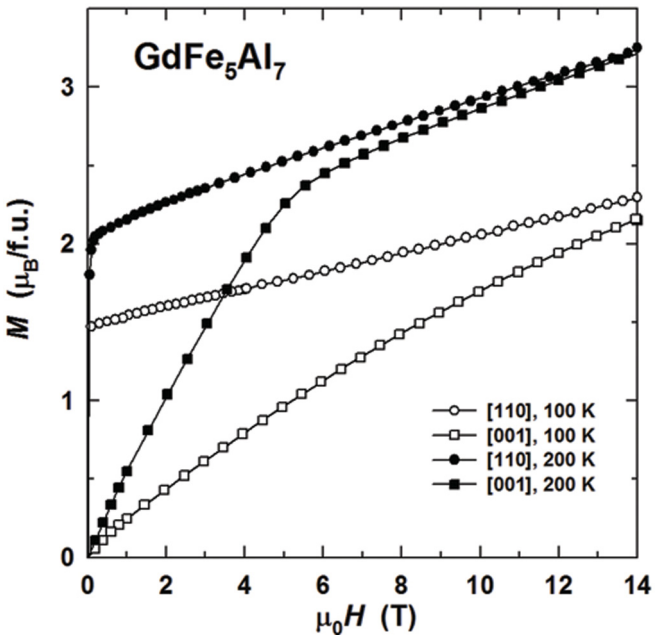


FIG. 2. Magnetization isotherms measured along the [110] and [001] axes of a $GdFe_5Al_7$ single crystal at 100 and 200 K.

## II. EXPERIMENTAL DETAILS

The $GdFe_5Al_7$ single crystal was prepared from a stoichiometric mixture of the elements (99.9% pure Gd, 99.98% pure Fe, and 99.999% pure Al) by a modified Czochralski method in a tri-arc furnace using a tungsten rod as a seed under 15-mm/h pulling speed. The obtained single crystal was 20-mm long and 3 mm in diameter. The back-scattered Laue patterns showed good quality of the crystal with misorientation of subgrains less than 1°. Phase purity and lattice parameters were determined by standard x-ray diffractometry in Cu $K\alpha$ radiation on a powder prepared from the single crystal. The diffraction patterns were refined by means of Rietveld analysis using the Fullprof/Winplotr software.[4] The lattice parameters, $a = 871.1$ pm, $c = 504.5$ pm, are in agreement with the literature.[5] Temperature and field dependence of magnetization was measured in static magnetic fields up to 14 T at temperatures between 4.2 and 300 K using a commercial magnetometer (Quantum Design PPMS)

## III. EXPERIMENTAL RESULTS

Figure 1 presents magnetization curves measured along the principal crystallographic axes at 2 K. (Theoretical fits shown in Fig. 1 will be introduced and discussed below.) One observes that [110] is the easy magnetization direction, the spontaneous magnetization at $T = 2$ K being

$$M_s = 0.58\ \mu_B/\text{f.u.} \tag{1}$$

There is also a nonzero projection of the spontaneous moment onto the [100] axis, 0.43 $\mu_B$/f.u. at $T = 2$ K. This is rather close to the expected value, $M_s/\sqrt{2} \approx 0.41\ \mu_B$/f.u., which reflects the high quality of the crystal and its proper orientation. The spontaneous moment has no component along [001], which is the hard magnetization direction. In Fig. 2, where magnetization curves at $T = 100$ and 200 K are presented, for clarity only the magnetization curves along the easy and the hard axes are shown, although the in-plane anisotropy survives up to 200 K (cf. Fig. 5).

After the domain-wall displacement is completed, the magnetization along the easy axis [110] continues to grow. The growth is approximately linear up to about 6 T (at $T = 2$ K), in accordance with the following expression:

$$M = M_s + \chi H, \tag{2}$$

where

$$\chi = 0.024\ \mu_B/\text{Tf.u.} \tag{3}$$

At the same time, the magnetization along [100] grows more rapidly and nonlinearly. At about 4T ($T = 2$ K) the magnetization curves along [100] and [110] intersect. Above 8 T all three curves are close to each other. The common high-field part at $T = 2$ K is linear and extrapolates to the origin according to the expression $M = \lambda^{-1}H$. Hence we determined the intersublattice exchange constant,

$$\lambda = 8.3\ \text{T f.u.}/\mu_B \tag{4}$$

as well as a dimensionless product,

$$\chi\lambda = 0.20. \tag{5}$$

Temperature dependence of magnetization measured in a field of 0.1 T applied along the three principal axes is presented in Fig. 3. In contrast to $DyFe_5Al_7$ and $HoFe_5Al_7$,[6,7] $GdFe_5Al_7$ has no compensation point because $M_{Fe} > M_{Gd}$ in the whole temperature range up to the Curie point $T_C$. Near $T_C$, the magnetization measured in a small but nonzero applied field deviates considerably from the true spontaneous magnetization, indicated by the open triangles in Fig. 3. The

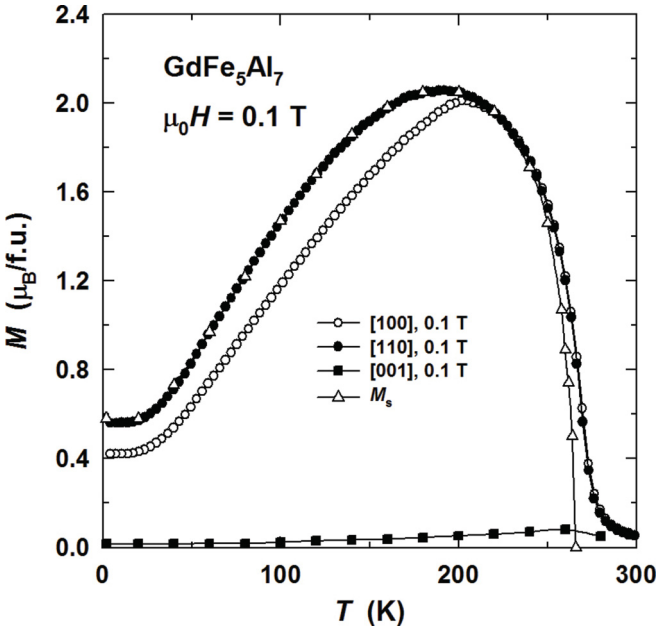


FIG. 3. Temperature dependence of magnetization along the [100], [110], and [001] axes measured in 0.1 T and temperature dependence of the spontaneous moment obtained from magnetization isotherms along the [110] axis.

latter was determined from the Arrott-Belov plots of Fig. 4(b) constructed from the magnetization isotherms shown in Fig 4(a). From the same plots we found the Curie temperature,

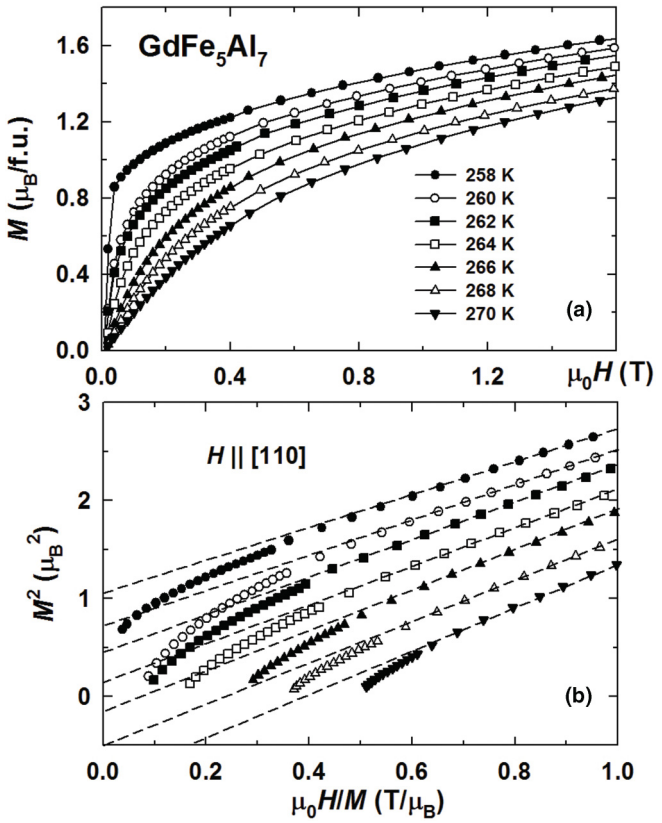


FIG. 4. Magnetization isotherms measured along the [110] axis in the vicinity of $T_C = 265$ K (a) and corresponding Arrott's plots (b).

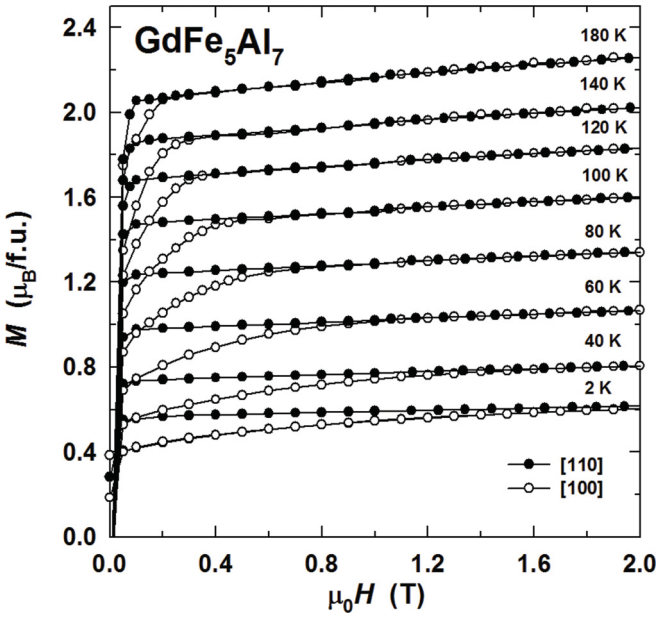


FIG. 5. Temperature evolution of the magnetization curves along the [100] and [110] axes of a $GdFe_5Al_7$ single crystal.

$$T_C = 265 \text{ K}. \quad (6)$$

Temperature evolution of the anisotropy between the [100] and [110] axes of the $GdFe_5Al_7$ single crystal is displayed in Fig. 5. The in-plane anisotropy field gradually decreases from 2 T at $T = 2$ K to about 0.2 T at $T = 180$ K and disappears at about 200 K. This can be also seen in Fig. 3, where the $M(T)$ curves in 0.1 T along [100] and [110] coincide above $T =$ 200 K.

Figure 6 shows in detail the magnetization isotherms along the [100] and [110] axes in the vicinity of the kink at $T = 20$ and 40 K. (The curves at $T = 2$ K are not shown since they are almost identical to those at 20 K.) At $T = 20$ K, an anisotropy of magnetization is observed between [100] and [110] above 5 T, where the bending of the sublattice moments results in a more rapid growth of the magnetization along [100]. As a result, in fields just above 5 T the magnetization along the easy [110] axis is lower. At 7 T it begins to grow more rapidly and above 8 T the two curves coincide. At $T = 40$ K the magnetization isotherms display similar features. Apart from the low-field region, the magnetization curves along [100] and [110] differ in the interval between 8 and 11 T. Above 40 K both magnetization isotherms look identical at all fields up to 14 T, except in the low-field region related to the in-plane anisotropy of $GdFe_5Al_7$.

Figure 7 shows magnetization isotherms measured along the hard axis [001]. The curves are linear below 100 K, but a change of slope emerges at $T = 120$ K at about 10 T, moving towards lower fields at higher temperatures.

## IV. THEORY

### A. General

We consider a two-sublattice ferrimagnet where one sublattice, with a moment of $\boldsymbol{M}_{\text{Gd}}$, consists of Gd atoms, whereas the other one, whose moment is $\boldsymbol{M}_{\text{Fe}}$, includes all iron atoms,

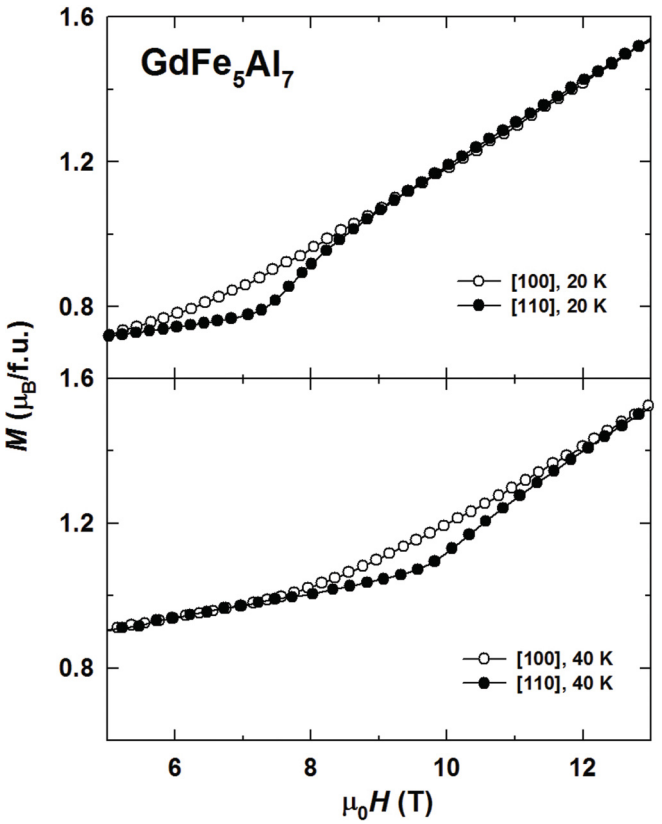


FIG. 6. Magnetization isotherms measured along the [100] and [110] axes of a $GdFe_5Al_7$ single crystal at $T = 20$ and 40 K.

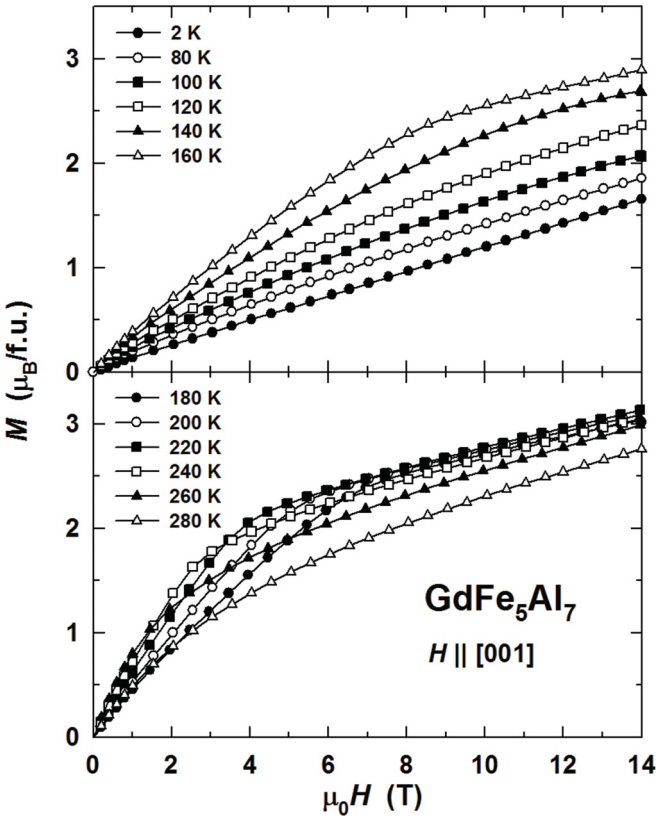


FIG. 7. Temperature evolution of the magnetization curve along the [001] axis of a $GdFe_5Al_7$ single crystal.

irrespective of their crystallographic position. Suppose $\boldsymbol{M}_{\mathrm{Fe}}$ and $\boldsymbol{M}_{\mathrm{Gd}}$ make angles $\alpha$ and $\beta$, respectively, with an applied magnetic field $\boldsymbol{H}$, as in Fig. 8. The system is at $T = 0$, so that the localized Gd sublattice is fully saturated, $|\boldsymbol{M}_{\mathrm{Gd}}| = \text{const.}$, but the itinerant Fe sublattice has a nonzero susceptibility. We proceed from the following thermodynamic potential:

$$\Phi = \lambda M_{\mathrm{Fe}} M_{\mathrm{Gd}} \cos(\alpha + \beta) - M_{\mathrm{Fe}} H \cos\alpha - M_{\mathrm{Gd}} H \cos\beta + \frac{1}{2\chi}(M_{\mathrm{Fe}} - M_0)^2 + K_{\mathrm{Fe}} \sin^2\alpha + K_{\mathrm{Gd}} \sin^2\beta + \ldots \quad (7)$$

Here the first term is the intersublattice exchange energy, $\lambda$ is the exchange constant as determined from the experiment (4). The second and third terms are the Zeeman energies of the sublattices.

The fourth term in Eq. (7) describes the stiffness of the iron sublattice; here $\chi$ is the susceptibility taken from the experiment [Eq. (3)], $M_0$ is a would-be equilibrium value of the iron moment $M_{\mathrm{Fe}}$ in the absence of intersublattice exchange and applied magnetic field. Thus, $M_{\mathrm{Fe}}$ is regarded as the system's internal thermodynamic parameter, to be determined by minimizing the potential $\Phi$. By contrast, $M_{\mathrm{Gd}}$ is believed to be a known constant, equal to the free-ion moment, $M_{\mathrm{Gd}} = 7\ \mu_{\mathrm{B}}$/f.u. It is important for the susceptibility of the iron sublattice $\chi$ to be small in relation to $\lambda^{-1}$,

$$\chi\lambda \ll 1. \quad (8)$$

Apparently, $GdFe_5Al_7$ does satisfy this condition [cf. Eq. (5)]. We intend to keep corrections linear in $\chi\lambda$ and $\kappa_{\mathrm{Fe}}$ [the latter being defined by Eq. (10) below] and neglect all higher-order terms.

The fifth and sixth terms in Eq. (8) are magnetic anisotropy energies of the sublattices. The suspension points imply that higher-order anisotropy terms could be appended, such as in $\sin^4\alpha$ and/or in $\sin^4\beta$. We have not yet chosen any particular orientation of the field $\boldsymbol{H}$, assuming merely that it points in a high-symmetry crystal direction. In certain situations the addition of a term in $\sin^4\alpha$ ($\sin^4\beta$) may be demanded by the symmetry, for example, when the sublattice moments rotate about a fourfold axis. (In such a case the prefactors of $\sin^2\alpha$ and $\sin^4\alpha$ must be equal in magnitude and opposite

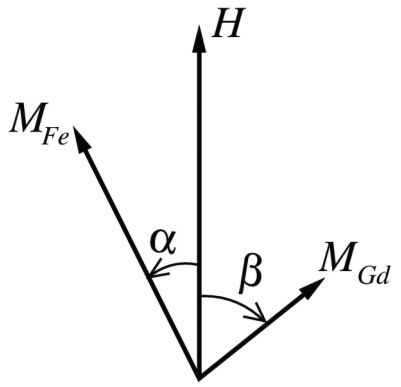


FIG. 8. Orientation of the magnetization vectors of the two sublattices with respect to the applied magnetic field. All vectors lie in the same plane.

in sign, in order for the correct functional dependence to arise, $\propto \cos 4\alpha$, see Sec. IV.) Anyhow, the anisotropy of the iron sublattice is supposed to be small in comparison to the intersublatice exchange energy,

$$|\kappa_{\mathrm{Fe}}| \ll 1, \tag{9}$$

where

$$\kappa_{\mathrm{Fe}} = (1 - \chi\lambda)\frac{K_{\mathrm{Fe}}}{\lambda M_0^2}. \tag{10}$$

Likewise, one can define a dimensionless anisotropy constant for the Gd sublattice,

$$\kappa_{\mathrm{Gd}} = (1 - \chi\lambda)\frac{K_{\mathrm{Gd}}}{\lambda M_0^2}. \tag{11}$$

We have reasons to believe that $\kappa_{\mathrm{Gd}}$ satisfies a strong inequality similar to Eq. (9). Yet, it is not postulated in this work that $\kappa_{\mathrm{Gd}}$ should be small. This is not necessary for the reduction of the present model to the model of rigid sublattices ($\chi = 0$), as long as the susceptibility of the rare earth sublattice can be neglected. Thus, the derivation (given in the Appendix) is also valid for rare earths other than Gd.

As one proceeds to minimizing Eq. (7) with respect to $\alpha$, $\beta$, and $M_{\mathrm{Fe}}$, one finds solutions of three distinct kinds.

(1) Ferrimagnetic: $\alpha = 0$, $\beta = \pi$, and

$$M_{\mathrm{Fe}} = M_0 + \chi H + \chi\lambda M_{\mathrm{Gd}}. \tag{12}$$

The magnetization of the ferrimagnetic phase is given by

$$M = M_{\mathrm{Fe}} - M_{\mathrm{Gd}} = M_s + \chi H, \tag{13}$$

where

$$M_s = M_0 - (1 - \chi\lambda)M_{\mathrm{Gd}}. \tag{14}$$

The ferrimagnetic phase should be stable in a low magnetic field applied along the easy axis. We identify this with the interval between 0 and 6 T in Fig. 1 ($\boldsymbol{H}\|[110]$). Our determination of $\chi$ from the slope of this part of the magnetization curve was in fact based on Eq. (13), which coincides with Eq. (2). The model parameter $M_0$ is found from Eq. (14) by using the experimental values of $M_s$ (1) and $\chi\lambda$ (5), as well as $M_{\mathrm{Gd}} = 7\ \mu_{\mathrm{B}}$/f.u.:

$$M_0 = 6.2\ \mu_{\mathrm{B}}/\mathrm{f.u.} \tag{15}$$

It is convenient to introduce a dimensionless reduced magnetization, $M/M_0$. For the ferrimagnetic phase one has

$$\frac{M}{M_0} = 1 - m + \frac{\chi\lambda}{1 - \chi\lambda}h, \tag{16}$$

where

$$m = (1 - \chi\lambda)\frac{M_{\mathrm{Gd}}}{M_0}, \quad h = (1 - \chi\lambda)\frac{H}{\lambda M_0}. \tag{17}$$

Hence

$$m = 0.907 \tag{18}$$

and

$$h = \frac{\mu_0 H}{64.3\ \mathrm{T}}. \tag{19}$$

(2) Ferromagnetic: $\alpha = \beta = 0$ and

$$M = M_0 + (1 - \chi\lambda)M_{\mathrm{Gd}} + \chi H. \tag{20}$$

The ferromagnetic phase is stable in very strong magnetic fields, not attained in our experiment.

(3) Canted: $\alpha$ and $\beta$ take general values, not fixed by the symmetry. The thermodynamic potential [Eq. (7)] has to be minimized with respect to all three internal parameters, $\alpha$, $\beta$, and $M_{\mathrm{Fe}}$. In general, the problem is very difficult, however, in the presence of the simplifying conditions (8) and (9) it is reduced to the model of rigid sublattices (see the Appendix). In doing so, two special cases should be distinguished, according to the orientation of the applied magnetic field.

### B. $\boldsymbol{H} \parallel [001]$

The parameter $K_{\mathrm{Fe}}$ in Eq. (7) is the conventional first anisotropy constant of the iron sublattice. The anisotropy of Gd is neglected: $K_{\mathrm{Gd}} = 0$ ($\kappa_{\mathrm{Gd}} = 0$) in Eqs. (7), (A3), and (A5). An estimate obtained in Eq. (25) below will justify the neglect *a posteriori*. (For comparison, a possible contribution of Gd could be ~0.4 K/atom, as inferred from Gd metal.[8,9]) The neglect of higher-order anisotropy constants is warranted by the example of an isomorphic $YFe_{11}Ti$.[10,11] The reduction to the model of rigid sublattices (see the Appendix) results in a system of simultaneous transcendental equations in $\alpha$ and $\beta$,

$$\begin{aligned} -m\sin(\alpha + \beta) + h\sin\alpha + \kappa_{Fe}\sin 2\alpha = 0, \\ -m\sin(\alpha + \beta) + mh\sin\beta = 0. \end{aligned} \tag{21}$$

The solution can be presented in a parametric form.[12] To this end, an auxiliary quantity is introduced,

$$t = \frac{2\cos\alpha}{h}, \tag{22}$$

which is used to express the reduced field,

$$h = \frac{1}{1 + \kappa_{\mathrm{Fe}}t}\sqrt{\frac{m^2 - (1 + \kappa_{\mathrm{Fe}}t)^2}{1 - t}}, \tag{23}$$

and reduced magnetization,

$$\frac{M}{M_0} = h\left(\frac{1 + \kappa_{\mathrm{Fe}}t}{1 - \chi\lambda} - \frac{\kappa_{\mathrm{Fe}}t^2}{2} - \frac{\chi\lambda}{1 - \chi\lambda}\frac{\kappa_{\mathrm{Fe}}h^2t^3}{4}\right). \tag{24}$$

Here $\chi\lambda$ and $m$ are known constants [Eqs. (5) and (18)], $t$ is a running parameter, and $\kappa_{\mathrm{Fe}}$ is an adjustable parameter. The best-fit value is $\kappa_{\mathrm{Fe}} = -0.04$. By Eq. (10), this corresponds to

$$K_{Fe} = -0.8\ \mathrm{MJ/m^3}, \quad \text{or} \quad -11\ \mathrm{K/f.u.} \tag{25}$$

The resulting magnetization curve is displayed in Fig. 1. The abscissas, found from Eq. (23), were converted to teslas by means of Eq. (19).

One observes that Eq. (24) is more complicated than the corresponding expression for reduced magnetization in the model of rigid sublattices. This is because the

magnetization,

$$M = M_{\mathrm{Fe}} \cos\alpha + M_{\mathrm{Gd}} \cos\beta, \tag{26}$$

now depends on $H$ not only through the angles $\alpha$ and $\beta$, but also through the module $M_{\mathrm{Fe}}$; cf. Eq. (A1). In the limit of rigid sublattices ($\chi \to 0$), Eq. (24) goes over—to a constant factor—into Eq. (A12) of Ref. 12.

In the isotropic limit ($\kappa_{\mathrm{Fe}} \to 0$), Eq. (24) becomes $M = \lambda^{-1} H$. This is the behavior observed above 8 T in Fig. 1, which justifies our determination of $\lambda$ from the high-field slope, Eq. (4).

It is worth noting that a nonzero $\chi$ cannot give rise to any additional reorientation transitions, because it does not enter into the field dependence of the sublattice orientation angles, as given by

$$\cos\alpha = ht/2, \quad \cos\beta = (h/m)(1 - t/2)(1 + \kappa_{\mathrm{Fe}} t), \tag{27}$$

in conjunction with Eq. (23).

### C. $H \perp [001]$

The sublattice vectors lie in the basal plane. To reflect the fourfold symmetry, Eq. (7) should be appended with a fourth-order Fe anisotropy term, $-K_{\mathrm{Fe}} \sin^4\alpha$. It is convenient to change to the conventional basal-plane anisotropy constant, $K'_{Fe} = -\frac{1}{8} K_{Fe}$, which is to multiply $\cos 4\alpha$. The anisotropy energy associated with the Gd sublattice can be neglected altogether. Estimates based on bcc iron[21] and $GdAl_2$,[22] $K'_{\mathrm{Fe}} \sim 6$ mK/atom and $K'_{\mathrm{Gd}} \sim 3$ mK/atom (that is, respectively, 30 and 3 mK/f.u.) will justify the neglect *a posteriori* [Eq. (31)]. The reduction to the model of rigid sublattices proceeds without complications and results in the following simultaneous equations:

$$\begin{aligned} -m\sin(\alpha+\beta) + h\sin\alpha \pm 4\kappa'_{\mathrm{Fe}} \sin 4\alpha = 0, \\ -m\sin(\alpha+\beta) + mh\sin\beta = 0, \end{aligned} \tag{28}$$

where $\kappa'_{\mathrm{Fe}}$ is a dimensionless anisotropy parameter, defined analogously to Eq. (10):

$$\kappa'_{\mathrm{Fe}} = (1 - \chi\lambda)\frac{K'_{\mathrm{Fe}}}{\lambda M_0^2} \tag{29}$$

The upper and lower signs in Eq. (28) correspond to the cases $\boldsymbol{H} \parallel [110]$ and $\boldsymbol{H} \parallel [100]$, respectively.

The simultaneous Eqs. (28) cannot be solved for $\alpha$ and $\beta$ analytically. So, the equilibrium angles had to be found numerically. Subsequently the magnetization was computed using Eqs. (A1) and (26). In actual fact, the thermodynamic potential was minimized numerically with respect to just one variable, $\alpha$ ($0 < \alpha < \pi/2$), $\beta$ being a known function of $\alpha$:

$$\beta = \frac{\pi}{2} - \arctan\frac{h - \cos\alpha}{\sin\alpha}. \tag{30}$$

This expression provides for the possibility of $\beta$ being obtuse and applies when the anisotropy is associated with the dominant sublattice. It should be distinguished from the more common case where the entire anisotropy is ascribed to the subdominant sublattice;[13–17] cf. Eq. (13) of Ref. 13.

The following best-fit value was obtained for the only adjustable parameter: $\kappa'_{\mathrm{Fe}} = 1.4 \times 10^{-4}$. This corresponds to

$$K'_{\mathrm{Fe}} \approx 3\mathrm{kJ/m^3}, \quad \text{or } 0.04\mathrm{K/f.u.} \tag{31}$$

### D. Spontaneous magnetization

Consider a case where the field is applied along the easy axis and $H \to 0$. The ferrimagnetic phase is stable, with $\alpha = 0$, $\beta = \pi$ and

$$M = M_s = M_{\mathrm{Fe}} - M_{\mathrm{Gd}}. \tag{32}$$

Let us lift the restriction $T = 0$. Now we have

$$M_{\mathrm{Gd}} = 7\mu_{\mathrm{B}} \mathrm{B}_{7/2}\left(\frac{7\mu_{\mathrm{B}}\lambda M_{\mathrm{Fe}}}{kT}\right), \tag{33}$$

$$M_{\mathrm{Fe}} = M_0 f_T + \chi\lambda M_{\mathrm{Gd}}. \tag{34}$$

Here $\mathrm{B}_{7/2}(x)$ is the Brillouin function for $S = 7/2$. The use of the Brillouin function implies neglect of the Gd-Gd exchange interaction, justified by Ref. 18. The phenomenological temperature factor $f_T$, such that $f_0 = 1$, describes the reduction of the iron sublattice's own moment with temperature. By contrast, the susceptibility $\chi$ is independent of temperature, as expected of itinerant electrons. At $T = 0$, Eq. (33) is just $M_{\mathrm{Gd}} = 7\mu_{\mathrm{B}}$; Eq. (34) is a special case of $H = 0$ in Eq. (12).

At $T \neq 0$ Eqs. (33) and (34) are solved by iterations, taking advantage of the strong inequality (8). In zeroth approximation, $\chi\lambda = 0$ and, by Eq. (34), $M_{\mathrm{Fe}} = M_0 f_T$. Then, by Eq. (33),

$$M_{\mathrm{Gd}} = 7\mu_{\mathrm{B}} \mathrm{B}_{7/2}\left(\frac{7\mu_{\mathrm{B}}\lambda M_0 f_T}{kT}\right), \tag{35}$$

whence, by Eq. (32),

$$M_s = M_0 f_T - 7\mu_{\mathrm{B}}(1 - \chi\lambda)\mathrm{B}_{7/2}\left(\frac{7\mu_{\mathrm{B}}\lambda M_0 f_T}{kT}\right). \tag{36}$$

The temperature factor is taken in the following form:

$$f_T = \left[1 - \left(\frac{T}{T_C}\right)^{3/2}\right]^{1/3}, \tag{37}$$

which is none other than Eq. (1) of Ref. 19 with $s = 1$. The dependence $M_s(T)$ computed by means of Eqs. (36) and (37) is plotted in Fig. 9 (solid line).

## V. DISCUSSION

Revising Figs. 1 and 9, one observes good agreement between the experimental data and theoretical fits. A system with nonzero $\chi$ has been described by using renormalized parameters in the model of rigid sublattices. The value [Eq. (4)] found for the intersublattice exchange constant of $GdFe_5Al_7$, $\lambda = 8.3$ T f.u./$\mu_{\mathrm{B}}$, is lower than that deduced from inelastic neutron scattering data for an isomorphic compound $GdFe_{10}Si_2$,[23] $\lambda = 12.2$ T f.u./$\mu_{\mathrm{B}}$. Yet, the difference is not unreasonable, given that $GdFe_{10}Si_2$ contains twice as many iron atoms per formula unit.

In the model, the anisotropy was ascribed entirely to the iron sublattice. This was done solely on the grounds

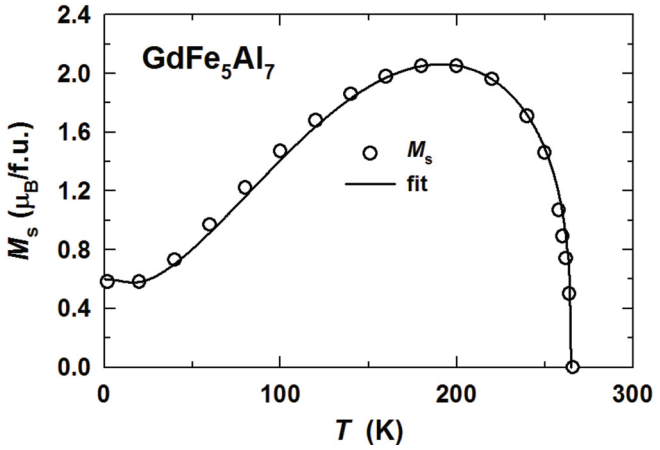


FIG. 9. Temperature dependence of the spontaneous magnetization of $GdFe_5Al_7$. The open circles are experimental data; the solid curve is a fit to Eqs. (36) and (37).

of plausibility, taking into consideration the smallness of a possible contribution of Gd to the overall anisotropy constants of $GdFe_5Al_7$ [Eqs. (25) and (31)]. The fits themselves provide no grounds for such a conclusion. In particular, an alternative model was tested, in which the basal-plane anisotropy had the same value [Eq. (31)] but was associated with the Gd sublattice. The resulting fits (not shown) differed little from those displayed in Fig. 1.

On the whole, the anisotropy within the basal plane has proved very weak in energy terms. It is rather surprising that this anisotropy is nonetheless clearly visible in $GdFe_5Al_7$, unlike in other tetragonal Gd-Fe or Y-Fe intermetallics. The reason is the near compensation of the sublattices in $GdFe_5Al_7$. This can be demonstrated most readily on the simplest model, regarding the sublattices as strictly antiparallel: The smallness of the first (axial) anisotropy constant $K_1$ does not necessarily mean that the anisotropy field, $H_a = 2K_1/|M_{Gd}-M_{Fe}|$, should be small, if $M_{Gd} \approx M_{Fe}$.

In a more refined approach, noncollinearity of the sublattice moments should be allowed for. For simplicity, we assume that all anisotropy energy is associated with the dominant sublattice, as relevant to $GdFe_5Al_7$. One should distinguish between the case of weak anisotropy,[12] when

$$|\kappa| < \frac{1}{2}(1-\sqrt{m})^2, \tag{38}$$

and the strong-anisotropy case, when the condition (38) is violated. (In the latter case the notion of "anisotropy field" is physically meaningless, as the magnetization curves in the easy and hard directions intersect without a phase transition.) The near compensation of the sublattices taking place in $GdFe_5Al_7$ means that the parameter $m$ is close to unity [cf. Eq. (18)]. Therefore, the right-hand side of the inequality (38) is very small, $\sim 1.1 \times 10^{-3}$. In spite of $|\kappa_{Fe}|$ being much less than unity ($\kappa_{Fe} = -0.04$), the condition (38) is still not fulfilled and the system is in the limit of strong anisotropy. This fact does not compromise in any way the reduction to the model of rigid sublattices (see the appendix), based on the strong inequalities (8) and (9).

Similar considerations, with some slight modifications, apply to the anisotropy in the basal plane. The value of anisotropy parameter found in Sec. IV C is very small, indeed, $\kappa'_{Fe} = 1.4 \times 10^{-4}$. This is, however, not small enough, on account of the near compensation. So, here as well the system operates in the strong-anisotropy regime, albeit not as far beyond the threshold. This is manifest in Fig. 1, where the magnetization curves along [100] and [110] intersect at 4 T without any anomaly, even though the former shows some inclination towards becoming N shaped. Another sign of proximity to the threshold of low anisotropy is that the half-area between the curves along [100] and [110] in Fig. 1 (left of their crossing point at 4 T), 3.4 kJ/m$^3$, is rather close to the corresponding anisotropy constant [Eq. (31)].

As regards the axial anisotropy of $GdFe_5Al_7$, it finds itself in the far strong-anisotropy limit [i.e., the threshold in the condition (38) is exceeded by $1\frac{1}{2}$ orders of magnitude]. A graphic manifestation of this is the absence of any remote hint at an N shape in the magnetization curve along [001] in Fig. 1. A further point of evidence is that the area between the curves along [110] and [001] underestimates the axial anisotropy constant [Eq. (25)] by as much as an order of magnitude.

## VI. CONCLUSION

The present magnetization study has demonstrated that $GdFe_5Al_7$ is a ferrimagnet with $T_C = 265$ K. The low-temperature spontaneous magnetization is rather small, $M_s = 0.58\ \mu_B$/f.u. at $T = 2$ K, that is, the system is in a state of near compensation. As a result, the magnetization curves show a significant apparent anisotropy, unexpected in a compound where none of the constituents has much of an orbital moment. All these facts find an explanation in a simple two-sublattice model. One of the peculiarities of $GdFe_5Al_7$ is that the iron sublattice has a non-negligible susceptibility which does not vanish as $T \to 0$. Yet, at $T = 0$ the model is reduced to the standard model of rigid sublattices with renormalized parameters. The calculated low-temperature magnetization curves and the temperature dependence of spontaneous magnetization are in good agreement with the experimental data.

## ACKNOWLEDGMENTS

This work has been supported by the Czech Science Foundation (Grant No. P204/12/0150). D.I.G. also acknowledges Charles University Grants No. SVV-2012-265303 and No. GAUK-703912.

## APPENDIX: REDUCTION TO THE MODEL OF RIGID SUBLATTICES

We proceed from necessary conditions for a minimum of the thermodynamic potential [Eq. (7)] with respect to the internal

parameters $M_{\mathrm{Fe}}$, $\alpha$, and $\beta$,

$$M_{\mathrm{Fe}} = M_0 + \chi[H\cos\alpha - \lambda M_{\mathrm{Gd}}\cos(\alpha+\beta)], \quad \text{(A1)}$$

$$-\lambda M_{\mathrm{Gd}}\sin(\alpha+\beta) + H\sin\alpha + \frac{K_{\mathrm{Fe}}}{M_{\mathrm{Fe}}}\sin 2\alpha + \ldots = 0, \quad \text{(A2)}$$

$$-\lambda M_{Fe} M_{\mathrm{Gd}}\sin(\alpha+\beta) + M_{\mathrm{Gd}} H\sin\beta + K_{\mathrm{Gd}}\sin 2\beta + \ldots = 0, \quad \text{(A3)}$$

where Eq. (A1) has been solved for $M_{\mathrm{Fe}}$ and Eq. (A2) has been divided by $M_{\mathrm{Fe}}$. The suspension points in Eqs. (A2) and (A3) indicate the possibility of including higher-order anisotropy terms.

The unknown $M_{\mathrm{Fe}}$ is eliminated from Eq. (A3) by setting therein Eq. (A1):

$$\begin{aligned}&-\lambda M_0 M_{\mathrm{Gd}}\sin(\alpha+\beta) - \chi\lambda M_{\mathrm{Gd}} H\sin(\alpha+\beta)\cos\alpha\\ &+\chi(\lambda M_{\mathrm{Gd}})^2\sin(\alpha+\beta)\cos(\alpha+\beta) + M_{\mathrm{Gd}} H\sin\beta\\ &+K_{\mathrm{Gd}}\sin 2\beta + \ldots = 0. \end{aligned} \quad \text{(A3a)}$$

Now the quantity $\lambda M_{\mathrm{Gd}}\sin(\alpha+\beta)$ is expressed from Eq. (A2) and substituted into the third term of Eq. (A3a):

$$\begin{aligned}&-\lambda M_0 M_{\mathrm{Gd}}\sin(\alpha+\beta) + (1-\chi\lambda)M_{\mathrm{Gd}} H\sin\beta\\ &+K_{\mathrm{Gd}}\sin 2\beta + \chi\lambda K_{\mathrm{Fe}}\frac{M_{\mathrm{Gd}}}{M_{\mathrm{Fe}}}\cos(\alpha+\beta)\sin 2\alpha + \ldots = 0. \end{aligned} \quad \text{(A3b)}$$

On foot of the inequalities (8) and (9), the last term in Eq. (A3b) can be neglected as a higher-order infinitesimal. To the same approximation, $M_{\mathrm{Fe}}$ in the denominator of the last term in Eq. (A2) can be replaced by $M_0$:

$$-\lambda M_{\mathrm{Gd}}\sin(\alpha+\beta) + H\sin\alpha + \frac{K_{\mathrm{Fe}}}{M_0}\sin 2\alpha + \ldots = 0, \quad \text{(A2a)}$$

$$\begin{aligned}&-\lambda M_0 M_{\mathrm{Gd}}\sin(\alpha+\beta) + (1-\chi\lambda)M_{\mathrm{Gd}} H\sin\beta\\ &+K_{\mathrm{Gd}}\sin 2\beta + \ldots = 0. \end{aligned} \quad \text{(A3c)}$$

Note that the inequality (8) need not be a strong one if $K_{\mathrm{Fe}} = 0$.

Equations (A2a) and (A3c) can be conveniently rewritten in terms of the dimensionless quantities defined by Eqs. (10), (11), and (17):

$$-m\sin(\alpha+\beta) + h\sin\alpha + \kappa_{Fe}\sin 2\alpha + \ldots = 0, \quad \text{(A4)}$$

$$-m\sin(\alpha+\beta) + mh\sin\beta + \kappa_{Gd}\sin 2\beta + \ldots = 0. \quad \text{(A5)}$$

Equations (A4) and (A5) are identical to the conditions for equilibrium in the model of rigid sublattices ($\chi = 0$), cf. Eqs. (5) and (6) of Ref. 20. The nonzero $\chi$ enters only into the definitions of the dimensionless variables, Eqs. (10), (11), and (17), but not into the equations for the angles $\alpha$ and $\beta$, Eqs. (A4) and (A5). Therefore, one can take over most of the results previously obtained within the model of rigid sublattices in all its variants, with or without $\kappa_{\mathrm{Fe}}$ and/or $\kappa_{\mathrm{Gd}}$, or perhaps with two anisotropy constants for the rare earth sublattice.[16] A special case of the latter version, with $\kappa_1 = -\kappa_2 = -8\kappa'$, describes a situation when the sublattices rotate about a fourfold symmetry axis.

*Corresponding author: gorbunov@fzu.cz


[1] M. Richter, in *Handbook of Magnetic Materials*, Vol. 13, edited by K. H. J. Buschow (North-Holland, Amsterdam, 2001), Ch. 2.

[2] W. Suski, in *Handbook on the Physics and Chemistry of Rare Earths*, Vol. 22, edited by K. A. Gschneidner Jr. and L. Eyring, (North-Holland, Amsterdam, 2001), Ch. 149.

[3] W. Kockelmann, W. Shäfer, G. Will, P. Fischer, and J. Gal, J. Alloys Compd. **207-208**, 311 (1994).

[4] http://www.ill.eu/sites/fullprof/.

[5] I. Felner, I. Nowik, and M. Seh, J. Magn. Magn. Mater. **38**, 172 (1983).

[6] D. I. Gorbunov, A. V. Andreev, and N. V. Mushnikov, J. Alloys Comp. **514**, 120 (2012).

[7] D. I. Gorbunov and A. V. Andreev, [Solid State Phenomena (in the press)].

[8] M. Colarieti-Tosti, S. I. Simak, R. Ahuja, L. Nordström, O. Eriksson, D. Åberg, S. Edvardsson, and M. S. S. Brooks, Phys. Rev. Lett. **91**, 157201 (2003).

[9] J. J. M. Franse and R. Gersdorf, Phys. Rev. Lett. **45**, 50 (1980).

[10] C. Abadía, P. A. Algarabel, B. García-Landa, M. R. Ibarra, A. del Moral, N. V. Kudrevatykh, and P. E. Markin, J. Phys.: Condens. Matter **10**, 349 (1998).

[11] S. A. Nikitin, I. S. Tereshina, V. N. Verbetskii, and A. A. Salamova, Phys. Solid State **40**, 258 (1998).

[12] D. I. Gorbunov, M. D. Kuz'min, K. Uhlířová, M. Žáček, M. Richter, Y. Skourski, and A. V. Andreev, J. Alloys Compd. **519**, 47 (2012).

[13] M. D. Kuz'min, Y. Skourski, K. P. Skokov, and K.-H. Müller, Phys. Rev. B **75**, 184439 (2007).

[14] A. V. Andreev, Y. Skourski, M. D. Kuz'min, S. Yasin, S. Zherlitsyn, R. Daou, J. Wosnitza, A. Iwasa, A. Kondo, A. Matsuo, and K. Kindo, Phys. Rev. B **83**, 184422 (2011).

[15] Y. Skourski, M. D. Kuz'min, K. P. Skokov, A. V. Andreev, and J. Wosnitza, Phys. Rev. B **83**, 214420 (2011).

[16] M. D. Kuz'min, J. Magn. Magn. Mater. **323**, 1068 (2011).

[17] E. A. Tereshina, I. S. Tereshina, M. D. Kuz'min, Y. Skourski, M. Doerr, O. D. Chistyakov, I. V. Telegina, and H. Drulis, J. Appl. Phys. **111**, 093923 (2012).

[18] M. D. Kuz'min, Y. Skourski, D. Eckert, M. Richter, K.-H. Müller, K. P. Skokov, and I. S. Tereshina, Phys. Rev. B **70**, 172412 (2004).

[19] M. D. Kuz'min, Phys. Rev. Lett. **94**, 107204 (2005).

[20] M. D. Kuz'min, J. Appl. Phys. **111**, 043904 (2012).

[21] R. M. Bozorth, J. Appl. Phys. **8**, 575 (1937). In order to change over to the tetragonal convention, the first anisotropy constant in the cubic notation, $K_1 = 5.7 \times 10^5$ erg/cm$^3$ at $T = 0$, should be multiplied by $-\frac{1}{8}$.

[22] J. Burd and E. W. Lee, J. Phys. C **10**, 4581 (1977).

[23] M. Loewenhaupt, P. Tils, K. H. J. Buschow, and R. S. Eccleston, J. Magn. Magn. Mater. **152**, 10 (1996).